Kidney International, Vol. 56 (1999), pp. 2025–2039

GENETIC DISORDERS – DEVELOPMENT

Expression and localization of fibroblast growth factors and fibroblast growth factor receptors in the developing rat kidney

Belinda Cancilla, Miriam D. Ford-Perriss, and John F. Bertram[1]

Department of Anatomy and Cell Biology, University of Melbourne, Parkville, and Institute of Reproduction and Development, Monash University, Clayton, Victoria, Australia

Expression and localization of fibroblast growth factors and fibroblast growth factor receptors in the developing rat kidney.

Background. The permanent kidney, or metanephros, develops through a complex series of reciprocal inductive events and involves branching morphogenesis, tubulogenesis, angiogenesis, and tissue remodeling. Fibroblast growth factors (FGFs) are a family of growth and differentiation factors that have been implicated in metanephric development. FGFs exert their actions through tyrosine kinase receptors, FGFRs, which are encoded by four FGFR genes (FGFR1 through FGFR4).

Methods. Reverse transcriptase-polymerase chain reaction was used to detect the expression of FGFs and FGFRs in rat metanephroi from embryonic day (E) 14 to E21. Nonradioactive *in situ* hybridization was used to localize FGF1 mRNA in E20 rat metanephroi, and immunohistochemistry was used to localize FGFRs in E15 and E20 rat metanephroi.

Results. We detected the expression of mRNAs for FGF1 through FGF5, FGF7 through FGF10, and FGFR1 through FGFR4 (IIIb and IIIc splice variants) in rat metanephroi from E14 to E21. By *in situ* hybridization, FGF1 mRNA was detected in the nephrogenic zone, ureteric epithelium, and developing nephron elements. FGFR proteins were localized in a distinct pattern that altered with maturation. FGFR1 was widely distributed in developing metanephric epithelia and mesenchyme, but not in developing interstitium. FGFR2 was also widely distributed in nephron epithelia, particularly in proximal convoluted tubules, but was not detected in metanephric mesenchyme, mesenchymal condensates, or developing interstitium. FGFR3 was localized to mesenchymal condensates, nephron elements, and medullary interstitium but not proximal convoluted tubules. FGFR4 was localized mostly to maturing nephron structures and was not detected in nephrogenic mesenchyme, mesenchymal condensates, or developing interstitium.

Conclusions. These results indicate that FGFs and FGFRs are expressed in the developing rat metanephros from at least E14 and that they likely play important roles in metanephric development and maturation.

[1] Current address: Department of Anatomy, Monash University, Clayton, Victoria, Australia.

Key words: growth factor, metanephros, kidney maturation, development, nephrogenic zone.

Received for publication December 1, 1998
and in revised form April 13, 1999
Accepted for publication July 19, 1999

The development of the permanent kidney, or metanephros, is a complex process involving reciprocal inductive events. In the first instance, the ureteric bud is induced to grow into the metanephric blastema. Ureteric epithelium induces mesenchymal condensation, whereas metanephric mesenchyme induces ureteric branching. The mesenchymal condensate converts to epithelium and differentiates through a comma-shaped body, S-shaped body, and capillary loop stage glomerulus to a maturing glomerulus [1]. The developing loop of Henle proceeds through three stages: (*a*) the primitive loop of Henle, which consists of thick undifferentiated epithelium; (*b*) the immature loop of Henle, which has thin immature epithelium in the descending portion and distal tubule epithelium in the ascending portion; and (*c*) the maturing loop of Henle, which consists of a thin limb and a distal straight tubule [2].

Many growth factors have been shown to play key roles in metanephric development [3–6], including members of the fibroblast growth factor (FGF) family. The FGF family has at least 19 members [7], only some of which have been examined in the kidney. FGF1 and FGF2 are present in both adult and embryonic kidneys, and crude kidney extracts have mitogenic and angiogenic activity caused by FGF2 [8]. Exogenous FGF2 can stimulate condensation of isolated rat metanephric mesenchyme *in vitro* [9], a critical early event in nephron development.

Previous studies have examined the expression of FGF1 [10], FGF2 [11], FGF7 [12], and FGF8 [13, 14] in human or rodent metanephroi. However, in these studies, only one developmental time point was examined. FGF2 mRNA has been localized to tubular epithelia, mesangial cells, and surrounding mesenchyme in human metanephroi at mid-gestation using radioactive *in situ* hybridization [11]. We have previously shown using immunohistochemistry that FGF1 and FGF2 are present from at least embryonic day 14 (E14) in rat kidneys [15]. We found that FGF1 and FGF2 were colocalized in metanephroi throughout gestation and in ureteric epithelium, glomeruli, and developing nephron tubules. Although

several studies have examined the localization of FGF1 protein in kidneys, these reports are conflicting. Therefore, we have used nonradioactive *in situ* hybridization to determine the localization of FGF1 mRNA in rat metanephroi.

The FGF family of ligands signals through specific transmembrane protein tyrosine kinase receptors (FGFRs). Efficient receptor dimerization and activation also require endogenous heparan sulfate proteoglycans (HSPGs), which avidly bind FGFs and facilitate their binding to FGFRs [16, 17]. During metanephric development, sulfated proteoglycans are initially produced at the ureteric bud tips. These then surround developing nephron elements and are found in basement membranes throughout the metanephros [18]. Four genes encode the FGFRs, which are characterized by three immunoglobulin-like (Ig) loops in the extracellular domain, a transmembrane region and a split intracellular tyrosine kinase domain [17]. Alternative mRNA splicing of the Ig-III domain of FGFR1 through FGFR3 gives rise to IIIb or IIIc FGFR variants. FGFR4 does not have alternative splicing of the Ig-III domain [17]. Studies on cell lines expressing a single type of FGFR variant have revealed that apart from FGF1, which activates all FGFRs, each FGF activates a particular subset of receptor variants [19, 20]. Consequently, the expression of a particular FGFR variant by a tissue/cell will determine to which FGF ligand that tissue/cell can respond.

Several studies have examined the expression of FGFRs in metanephroi. Northern blot analysis of 17- to 18-week-old human fetal tissues demonstrated that FGFR1, FGFR2, FGFR3, and FGFR4 mRNAs are present in developing human kidneys [21]. Splice variants in loop I and loop II of FGFR1 are expressed in rat metanephroi and were detected by reverse transcriptase-polymerase chain reaction (RT-PCR) at E14, E17, and E20 [22]. FGFR1, FGFR3, and FGFR4 have also been detected by RT-PCR in E21 rat kidneys [23].

Fibroblast growth factor receptor 1 mRNA has been localized in rat [24] and mouse [25, 26] metanephroi in condensates and comma- and S-shaped bodies, and some localization was also detected in ureteric bud branches. In human metanephroi, FGFR1 protein and mRNA have been localized in renal tubules and early nephron structures [11]. FGFR2 expression has been localized in collecting ducts and some nephron tubules of mouse embryos [25, 26].

In situ hybridization for FGFR3 IIIb and IIIc splice variants detected mRNA for IIIb but not IIIc in urinary tract epithelia of E14 and E20 mouse embryos, although the metanephros was not examined [27]. *In situ* hybridization studies on the expression pattern of FGFR4 in murine development have shown that it is expressed in a number of tissues, including metanephroi [28, 29]. Within metanephroi, FGFR4 mRNA was found in collecting tubules at E14.5.

Previous studies have not determined when FGFR2, FGFR3, or FGFR4 are first expressed in rat metanephroi and have not determined which IIIb or IIIc FGFR variants are present. Although several *in situ* hybridization studies have reported localization of FGFR mRNAs in metanephroi, localization of FGFR protein has only been studied for FGFR1 in human tissues.

In this study, we have shown using RT-PCR that mRNAs for FGF1 through FGF5, FGF7 through FGF10 are present in rat metanephroi from E14 to E21. To complement this work and to add to our previous localization studies of FGF2 [15], we have used nonradioactive *in situ* hybridization histochemistry to localize the expression of FGF1 in E20 rat metanephroi. With RT-PCR, we have shown that mRNAs for FGFR1 through FGFR4 are present in rat metanephroi from E14 to E21, and in addition, we have also determined which IIIb or IIIc FGFR variants were expressed and the onset of their expression. Finally, avidin-biotin–enhanced indirect immunohistochemistry was used to localize FGFR1 through FGFR4 proteins in E15 and E20 rat metanephroi. Together, these data provide a basis for future functional studies into the roles of FGFs in developing metanephroi. In light of the preference of particular FGFs for signaling through specific FGFR variants, the localization of FGFRs to specific nephron compartments suggests that these regions may be targets for particular FGFs. They indicate that other members of the FGF family, in addition to the well-studied FGF1 and FGF2, may play important roles in kidney development.

METHODS

Animals

Pregnant time-mated female Sprague-Dawley rats were anesthetized with an intraperitoneal injection of pentobarbitone sodium (Nembutal; Boehringer Ingelheim, Artarmon, NSW, Australia) at 5 mg/100 g body wt. A midline abdominal incision was made, and the uterus was located. Fetal rats were removed from the uterus, detached from the placenta, and quickly decapitated. The mothers were euthanized, and a sample of skeletal muscle was removed for positive control RNA. Metanephroi were dissected from fetal rats at each day of gestation from E14 to E21. E0 was defined as the time ($\pm$1 hr) at which the vaginal plug was found, and fetuses were dissected at or close to this time of day. All animal experiments were approved by the University of Melbourne Animal Experimentation Ethics Committee and were in accordance with the *Australian Code of Practice for the Care and Use of Animals for Scientific Purposes.*

For isolation of mRNA for RT-PCR, metanephroi were dissected from two sets of 24 fetal rats at each age

from E14 to E21 and were snap frozen in liquid nitrogen; skeletal muscle was collected from two females. Total RNA was isolated using TRIzol reagent (Life Technologies, Gaithersburg, MD, USA) following the manufacturer's instructions. mRNA was then isolated from the metanephric RNA using the PolyATract mRNA Isolation System (Promega, Madison, WI, USA) following the manufacturer's instructions, and the resulting pellet was resuspended in 20 μl of RNase-free water. For immunohistochemistry, metanephroi were fixed in Bouin's fixative for four hours and processed into paraffin, and 3 μm serial sections were cut. Two mothers (with 12 fetuses each) were used, and immunohistochemistry was performed on two sets of serial sections from each set of fetal rats. For *in situ* hybridization, metanephroi were fixed in 4% paraformaldehyde for two hours and were processed into paraffin, and 5 μm serial sections were cut.

Reverse transcriptase-polymerase chain reaction

Reverse transcription and PCR were performed sequentially in the same reaction tube using GeneAmp RNA PCR kit (Perkin Elmer, Foster City, CA, USA) according to manufacturer's instructions. Reverse transcription was performed with 2 μl isolated mRNA (or total RNA) and 100 ng appropriate reverse primer to generate cDNA.

Oligonucleotide primers used for amplification of FGF1 were p8 (reverse) and p9 (forward), with p10 as the internal oligonucleotide [30]. For amplification of FGF2, p1 (forward) and p2 (reverse) were used [31], with Ra1 [32] as the internal oligonucleotide used for Southern analysis. For amplification of FGF3, the primers used were forward (5′-GTGGCGTTTACGAGCACCTC), internal (5′-GAACAAGAGAGGACGGCTG), and reverse (5′-CACCGACACGTACCAAGGTC). For amplification of FGF4, the primers used were forward (5′-CAGTCTTCTGGAGCTCTCTC), internal (5′-ACTGAGGGCCATGAACATAC), and reverse (5′-GTTACCTTCATGGTAGGCGAC). For amplification of FGF5, primers used were forward (5′-TCGGTTTCCATCTGCAGATC), internal (5′-GCTGAACTTACAGTCATCTGTA), and reverse (5′-CTGGAACAGTGACGGTGAAG). For amplification of FGF6, the primers used were forward (5′-CTCGTCTTCTTAGGCGTCCT), internal (5′-CTACTGGACTCCAGAGGCTG), and reverse (5′-CCGTCCATATTTGCTCAGTG). For amplification of FGF7, the primers used were forward (5′-CCGACTCCGCTCTACAGACC), internal (5′-TGTTCTGTCGCACCCAGTGG), and reverse (5′-GTTGCAATCCTCATTGCATTC). For amplification of FGF8, the primers used were forward (5′-ACAAGCGCATCAACGCCATG), internal (5′-GGCAGGCGCTTCATGAAGTG), and reverse (5′-GGCGGGTAGTTGAGGAACTC). For amplification of FGF9, the primers used were forward (5′-AGGCAGCTGTACTGCAGGAC), internal (5′-TCTGGTGCCGTTTAGTCCTG), and reverse (5′-TAGTTCAGGTACTTTGTCAGG). For amplification of FGF10, the primers used were forward (5′-ACATTGTGCCTCAGCCTTTC), internal (5′-CATGGTGTCACCGGAGGCTA), and reverse (5′-TTCCATTCAATGCCACATACAT). Oligonucleotide primers used for amplification of FGFR1 through FGFR4 transmembrane domains and FGFR1 through FGFR3 IIIb and IIIc variants were identical to those used previously for amplification from adult rat kidney [32].

After reverse transcription, 100 ng of forward primer and an Ampliwax gem (Perkin Elmer) were added to the cDNA, and the reaction tube was then heated and cooled to allow a solid layer of wax to form over the samples. PCR components were then added to the cDNA, and the samples were heated to 95°C for 120 seconds to allow the wax to melt and cDNA and the PCR components to mix. PCR conditions were denaturation at 95°C, annealing at 55°C or 60°C, and extension at 72°C for 60 seconds each for 35 cycles. The controls used for RT-PCR were to replace the RT with water (non-RT control) and to replace mRNA with water (H_2O control).

Reverse transcriptase-PCR products were electrophoresed through 1.4% agarose gels and then alkaline capillary blotted onto Hybond N+ membrane (Amersham, Little Chalfont, Buckinghamshire, UK) as described in Sambrook, Fritsch, and Maniatis [33]. RT-PCR products were detected by hybridization at 42°C for 18 hours with their respective internal oligonucleotides, which were radioactively labeled by 5′ end labeling using [γ-^{32}P]-adenosine 5′-triphosphate ([γ-^{32}P]-ATP; Amersham) and T4 polynucleotide kinase (Boehringer Mannheim, Castle Hill, NSW, Australia). After stringent washes [to 0.5 × standard saline citrate (SSC), 0.1% sodium dodecyl sulfate (SDS) at 42°C], membranes were exposed to autoradiographic film. The identity of most of the FGF and all of the FGFR RT-PCR products detected by Southern analysis was confirmed by direct sequencing of PCR products on an automated ABI 310 Prism DNA sequencer (Applied Biosystems, Melbourne, Australia).

Riboprobe production

Fibroblast growth factor 1 cDNA clones were derived as previously described [30]. RT-PCR products for FGF1 (approximately 160 bp) were blunt-end ligated into the *Sma*I restriction site of pGEM-3Zf(+) vectors (Promega). Plasmids used for further experiments contained inserts oriented such that T7 RNA polymerase would produce sense FGF1 cRNA and SP6 RNA polymerase would produce antisense FGF1 cRNA. Plasmids were linearized with *EcoR*I (for antisense riboprobes) or *Sal*I (for sense riboprobes) restriction endonucleases (Boehringer Mannheim). *In vitro* transcription of biotin-UTP–labeled cRNA probes with T7 and SP6 RNA polymer-

ases was performed using the Riboprobe Gemini II System (Promega) following the manufacturer's instructions, with replacement of rUTP with 1 μl 20 mM biotin-21-rUTP (Clontech, Palo Alto, CA, USA). The relative size and concentration of the probes were assessed by Northern blot analysis (data not shown).

In situ hybridization

Nonradioactive *in situ* hybridization was performed on sections of rat metanephroi from E20 fetuses as previously described [34]. Briefly, paraffin sections were dewaxed, rehydrated, and then treated with 0.1 M glycine, 0.3% Triton X-100, digested with 50 μg/ml proteinase K (Promega) at 37°C for 30 minutes, postfixed in 4% paraformaldehyde in phosphate-buffered saline, and treated with 0.25% acetic anhydride. Sections were prehybridized [in 50% formamide, 2 × SSC, 0.3% bovine serum albumin (BSA) and 1 mg/ml tRNA] at 42°C for one hour. Fifty to 100 ng of biotin-UTP–labeled cRNA probe were denatured at 75°C for five minutes in 20 μl hybridization buffer [50% formamide, 2 × SSC, 10% polyethylene glycol (PEG), 0.3% BSA, 0.5% SDS, 0.25% polyvinylpyrrolidone, 0.02% Ficoll 400, 0.3% Triton X-100, 0.25 M Tris (pH 7), and 500 μg/ml tRNA] and cooled on ice, and then 20 U RNasin (Promega) was added. Prehybridization solution was then drained from the slide, and the probe solution was added. A cover slip was placed over the section, and the edges were sealed with rubber cement. Sections were then hybridized in a humid chamber at 42°C overnight. The cover slip was removed the next day by soaking the slide in 2 × SSC. Sections were then washed twice in 2 × SSC at 42°C for 10 minutes each, followed by two washes in phosphate-buffered saline at 42°C for 10 minutes each. A blocking solution of 2% BSA, 0.3% Triton X-100 in Tris-buffered saline (TBS; 0.9% NaCl in 0.1 M Tris, pH 7.4) was applied for 30 minutes. Sections were then incubated in an avidin-biotin horseradish peroxidase complex (Vectastain Elite ABC kit; Vector Laboratories, Burlingame, CA, USA) for one hour, followed by two washes with 0.3% Triton X-100 in TBS; they were then washed once with TBS. Sections were reacted to color with 0.5 mg/ml diaminobenzidine (Sigma Chemical Co., St. Louis, MO, USA) and 0.01% H_2O_2 in TBS. The reaction was stopped with water, and sections were dehydrated, cleared, and mounted.

Immunohistochemistry

Immunohistochemistry was performed as previously described [35]. Briefly, sections were dewaxed, rehydrated, and digested in 0.02% trypsin solution (Commonwealth Serum Laboratories, Melbourne, Australia) for 30 minutes at room temperature. Sections were then treated with 6% H_2O_2 for 10 minutes to remove endogenous peroxidase activity. After blocking for one hour, primary antibodies were incubated on sections overnight at 4°C. Antibodies were detected by incubation with biotinylated secondary antibody (Vector Laboratories) for one hour, followed by incubation with avidin-biotin horseradish peroxidase complex (Vectastain Elite ABC kit; Vector Laboratories) for one hour and reacted to color with diaminobenzidine (Sigma Chemical).

Affinity-purified rabbit polyclonal antibodies raised to peptides mapping at the carboxy-terminus of FGFR1 (residues 808 to 822 of the human *flg* gene product), FGFR2 (residues 805 to 821 of the human *bek* gene product), FGFR3 (residues 792 to 806 of human FGFR3), and FGFR4 (residues 789 to 802 of human FGFR4) were purchased from Santa Cruz Biotechnology (Santa Cruz, CA, USA) and used at 0.5 μg/ml. Each FGFR antibody was tested by immunoprecipitation and Western blotting by Santa Cruz Biotechnology, and cross-reactivity with other FGFRs was not detected. These antibodies cannot discriminate between the IIIb and IIIc functional variants of each receptor and will, therefore, detect both variants if present in the tissue. Control sections in this study were incubated with rabbit serum (Sigma Chemical) or with antibodies that had been preabsorbed with 2 μg/ml immunizing peptides (Santa Cruz Biotechnology).

RESULTS

Reverse transcriptase-polymerase chain reaction

RT-PCR for FGF1 through FGF10. RT-PCR indicated that mRNAs for FGF1 (307 bp RT-PCR product), FGF2 (355 bp RT-PCR product), FGF3 (372 bp RT-PCR product), FGF4 (261 bp RT-PCR product), FGF5 (414 bp RT-PCR product), FGF7 (384 bp RT-PCR product), FGF8 (384 bp RT-PCR product), FGF9 (411 bp RT-PCR product), and FGF10 (548 bp RT-PCR product) were present in metanephroi from E14, E17, and E21 rat embryos (Fig. 1). FGF6 (492 bp RT-PCR product) was expressed in the positive control skeletal muscle but was not expressed in rat metanephroi. No RT-PCR products were detected in the H_2O or non-RT controls of any sample. The results are summarized in Table 1.

RT-PCR for FGFR1 through FGFR4 (tm) transmembrane domain. RT-PCR indicated that mRNAs for FGFR1 (446 bp RT-PCR product), FGFR2 (452 bp RT-PCR product), FGFR3 (431 bp RT-PCR product), and FGFR4 (434 bp RT-PCR product) were present in E14, E17, and E21 rat metanephroi (Fig. 2). No RT-PCR products were detected in the H_2O or non-RT controls, with the exception of FGFR3, in which small amounts of contaminating genomic DNA (approximately 950 bp product) were amplified in the non-RT control sample of E21 metanephroi. The results are summarized in Table 2.

RT-PCR for FGFR1 through FGFR3 IIIb and IIIc variants. RT-PCR indicated that mRNAs for FGFR1 IIIb (350 bp RT-PCR product), FGFR1 IIIc (348 bp RT-

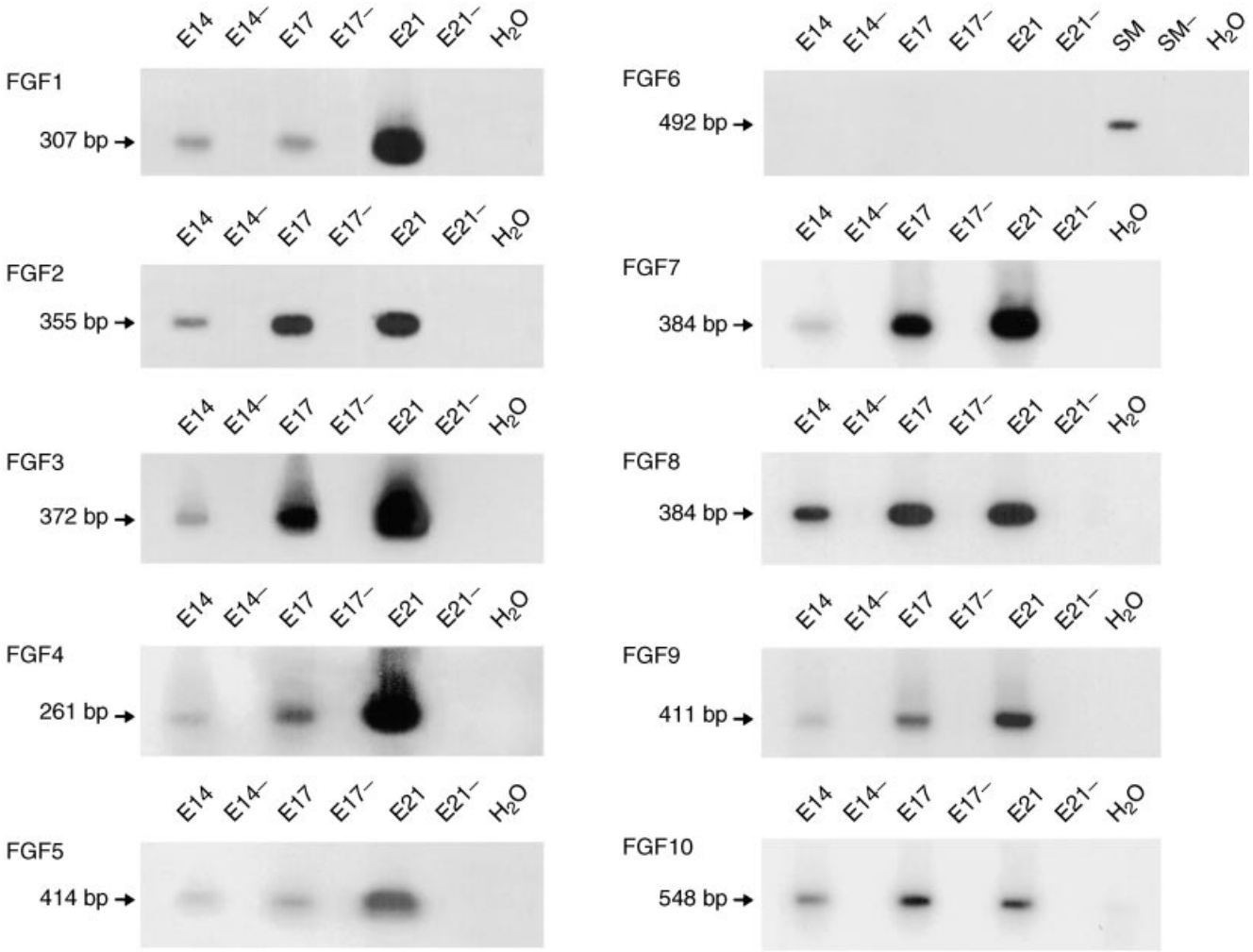

Fig. 1. Southern analysis of RT-PCR products for fibroblast growth factors (FGFs) generated from rat metanephric mRNA from embryonic day 14 (E14), E17, and E21. For each age, the non-RT controls are labeled with "−". The water control is labeled H_2O. RT-PCR products for FGF1 through FGF5 and FGF7 through FGF10 are present in metanephroi at all ages examined. FGF6 was expressed in the positive control adult skeletal muscle (SM) but not in metanephroi at any age examined.

Table 1. Summary of RT-PCR detection of fibroblast growth factor (FGF) expression in rat metanephroi

FGF mRNA	E14	E17	E21
FGF1	+	+	+
FGF2	+	+	+
FGF3	+	+	+
FGF4	+	+	+
FGF5	+	+	+
FGF6	−	−	−
FGF7	+	+	+
FGF8	+	+	+
FGF9	+	+	+
FGF10	+	+	+

Symbols are: +, expressed; −, not expressed.

PCR product), FGFR2 IIIb (360 bp RT-PCR product), FGFR2 IIIc (318 bp RT-PCR product), and FGFR3 IIIc (331 bp RT-PCR product) were present in metanephroi from E14, E17, and E21 rat embryos (Fig. 3). In contrast, FGFR3 IIIb mRNA (351 bp RT-PCR product) was not expressed in metanephroi until E16. No RT-PCR products were detected in the H_2O or non-RT controls of any sample. The results are summarized in Table 3.

Localization of FGF1 mRNA

Fibroblast growth factor 1 mRNA was detected in several regions of the developing rat metanephros (Fig. 4A). FGF1 mRNA was detected throughout the ureteric epithelium from the developing papilla to the ureteric bud tips in the nephrogenic zone (Fig. 4A). Nephrogenic zone mesenchyme and early nephron elements, including condensates, comma- and S-shaped bodies, also contained mRNA for FGF1. Expression of FGF1 mRNA appeared to decrease with glomerular maturation, with a strong signal detected in early capillary loop stage

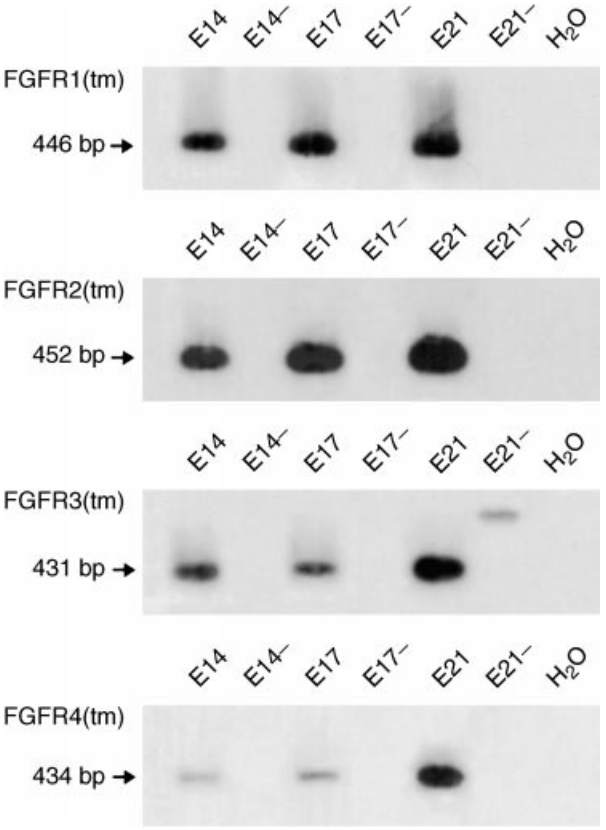

Fig. 2. Southern analysis of RT-PCR products for fibroblast growth factor receptor (FGFR) transmembrane (tm) domain generated from E14, E17, and E21 rat metanephric mRNA. For each age, the non-RT controls are labeled with "−" and the water control is labeled H_2O. RT-PCR products for FGFR1, FGFR2, FGFR3, and FGFR4 are present in metanephroi at all ages examined.

Table 2. Summary of RT-PCR detection of fibroblast growth factor receptor (FGFR) transmembrane (tm) domain expression in rat metanephroi

FGFR (tm)	E14	E17	E21
FGFR1	+	+	+
FGFR2	+	+	+
FGFR3	+	+	+
FGFR4	+	+	+

Symbols are: +, expressed; −, not expressed.

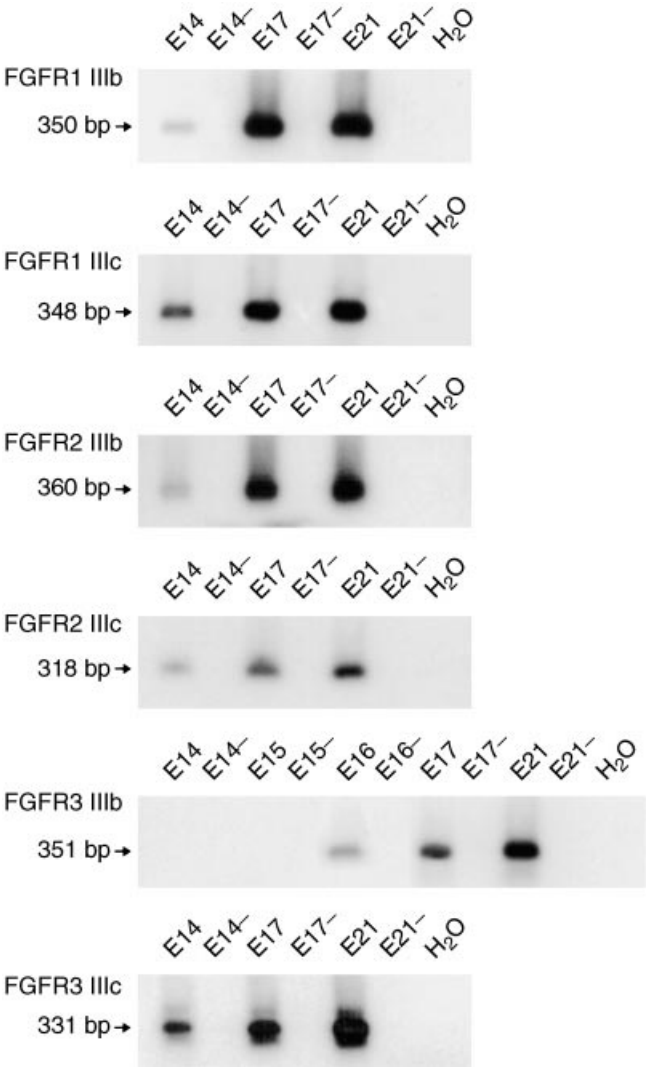

Fig. 3. Southern analysis of RT-PCR products for FGFR1 through FGFR3 IIIb and IIIc variants generated from rat metanephric mRNA from E14 through E17 and E21. For each age, the non-RT controls are labeled with "−" and the water control is labeled H_2O. RT-PCR products for FGFR1 IIIb and IIIc, FGFR2 IIIb and IIIc, and FGFR3 IIIc are present in metanephroi from E14-E21. RT-PCR products for FGFR3 IIIb are not present in E14 or E15 metanephroi but are present from E16 through E21.

glomeruli, but less expression in maturing stage glomeruli located at the corticomedullary boundary (Fig. 4A). All parts of S-shaped bodies expressed FGF1 mRNA. This pattern altered with tubular development, with only background levels of signal detectable in developing proximal tubules and in the thin undifferentiated epithelium of the immature loop of Henle, but with an intense signal observed in developing distal straight and convoluted tubules (Fig. 4A). No FGF1 mRNA was detected in the developing interstitium or in endothelium. No signal was detected in the corresponding section hybridized with sense cRNA probe (Fig. 4B).

To determine whether the strong signal observed in the nephrogenic zone was due to edge artifact, some E20 metanephroi were sliced in half prior to embedding in paraffin. Sections were then hybridized under the same conditions as those described earlier in this article. In these sections, no signal was detected in the interstitium along the cut edge of the metanephros (data not shown), and the pattern of cRNA hybridization in nephron structures was identical to that described earlier in this article in complete sections. This indicates that the signal de-

Table 3. Summary of RT-PCR detection of fibroblast growth factor receptor (FGFR) variant expression in rat metanephroi

FGFR variant	E14	E15	E16	E17	E21
FGFR1(IIIb)	+	nd	nd	+	+
FGFR1(IIIc)	+	nd	nd	+	+
FGFR2(IIIb)	+	nd	nd	+	+
FGFR2(IIIc)	+	nd	nd	+	+
FGFR3(IIIb)	−	−	+	+	+
FGFR3(IIIc)	+	nd	nd	+	+

Symbols are: +, expressed; −, not expressed; nd, not determined.

tected in the developing nephrogenic zone and cortex was not an edge artifact.

Immunohistochemistry

Immunohistochemistry was performed on E15 and E20 rat metanephroi. A distinct pattern of immunostaining was detected for each FGFR. In E15 metanephroi, FGFR1 was localized to mesenchymal condensates and ureteric epithelium, with weak localization in the metanephric mesenchyme (Fig. 5A). FGFR2 was localized to the ureteric epithelium, with very little staining in the metanephric and condensing mesenchyme (Fig. 5B). The distribution of FGFR3 was similar to FGFR1, with localization in ureteric epithelium and mesenchymal condensates, but not in the surrounding metanephric mesenchyme (Fig. 5C). Localization of FGFR4 was similar to FGFR2, with immunoreactivity exclusively in the ureteric epithelium at E15 (Fig. 5D). No specific immunostaining was observed in sections incubated with diluent or with rabbit serum (data not shown). Preabsorption of FGFR antibodies with immunizing peptides abolished the immunostaining pattern observed for each antibody (Fig. 5E for FGFR1, Fig. 5F for FGFR2, Fig. 5G for FGFR3, and Fig. 5H for FGFR4).

The overall differences in localization of each receptor at E20 can easily be observed in low-power photomicrographs (Fig. 5 I–L). In brief, FGFR1 immunoreactivity was detected in several structures throughout the metanephros, including the ureteric epithelium and the nephrogenic zone (Fig. 5I). FGFR2 immunoreactivity was detected primarily in proximal convoluted tubules and the ureteric epithelium (Fig. 5J). FGFR3 was detected in the nephrogenic zone and developing cortex but was absent from the ureteric epithelium of the developing medulla, where nephron tubules were immunoreactive (Fig. 5K). FGFR4 immunoreactivity was present in ureteric epithelium, but was primarily localized in maturing nephron epithelia (Fig. 5L). No specific immunostaining was observed in sections incubated with diluent, rabbit serum (data not shown) or with preabsorbed FGFR antibodies (Fig. 5M for FGFR1, Fig. 5N for FGFR2, Fig. 5O for FGFR3, and Fig. 5P for FGFR4). A detailed description of the localization of each FGFR follows.

Fibroblast growth factor receptor 1

Immunostaining for FGFR1 was localized in many structures of the developing E20 metanephros. Immunoreactivity for FGFR1 was seen in ureteric epithelium of the developing cortex and medulla (Fig. 5I). In the nephrogenic zone, the nephrogenic mesenchyme was immunoreactive for FGFR1 (Fig. 6A). Significantly, immunostaining for FGFR1 was localized in condensing mesenchymal cells at the tips of the ureteric branches (Fig. 6A), indicating that these cells have the capacity to respond to FGFs. This localization was maintained in developing nephron elements, where comma- and S-shaped bodies were immunoreactive for FGFR1 (Fig. 6B).

In maturing nephrons, FGFR1 was localized in capillary loop and maturing stage glomeruli (Fig. 6C) and appeared to be in podocytes, mesangial cells, and glomerular endothelium. Developing nephron tubules also demonstrated specific immunostaining for FGFR1, with immunoreactivity localized in proximal and distal convoluted tubules (Fig. 6C); some cross-sections through proximal convoluted tubules were only weakly stained. Both the descending and ascending limbs of the primitive loop of Henle and the immature loop of Henle (Fig. 6D) were immunostained for FGFR1. Immunoreactivity for FGFR1 was also detected in capillary endothelium, but not in the developing interstitium (Fig. 6D). FGFR1 was also localized in the endothelium of developing blood vessels and in the tunica media of arteries. The localization of FGFR1 in rat metanephric structures is summarized in Table 4.

Fibroblast growth factor receptor 2

Immunoreactivity for FGFR2 in the E20 metanephros was more restricted than that of FGFR1. The ureteric epithelium of the developing cortex and medulla was immunostained for FGFR2 (Fig. 5J), as was the case for FGFR1. However, in the nephrogenic zone, FGFR2 immunoreactivity was not detected in nephrogenic mesenchyme, condensates, comma- or S-shaped bodies (Fig. 6 E, F). Weak immunostaining was detected in the lower limbs of late S-shaped bodies (glomerular anlage), and this localization was maintained in developing glomeruli with immunostaining for FGFR2 observed in capillary loop and maturing-stage glomeruli (Fig. 6G). In maturing-stage glomeruli, localization appeared to be in podocytes and mesangial cells but not in endothelium.

In developing nephron tubules, intense immunostaining was observed in maturing proximal tubules (Fig. 6G), with weaker staining in distal tubules. In the developing loop of Henle, immunostaining for FGFR2 was localized throughout the primitive loop. With further development, strong staining was detected in the thin undifferentiated epithelium of the immature loop of Henle (Fig. 6H), with weaker staining in the ascending distal limb.

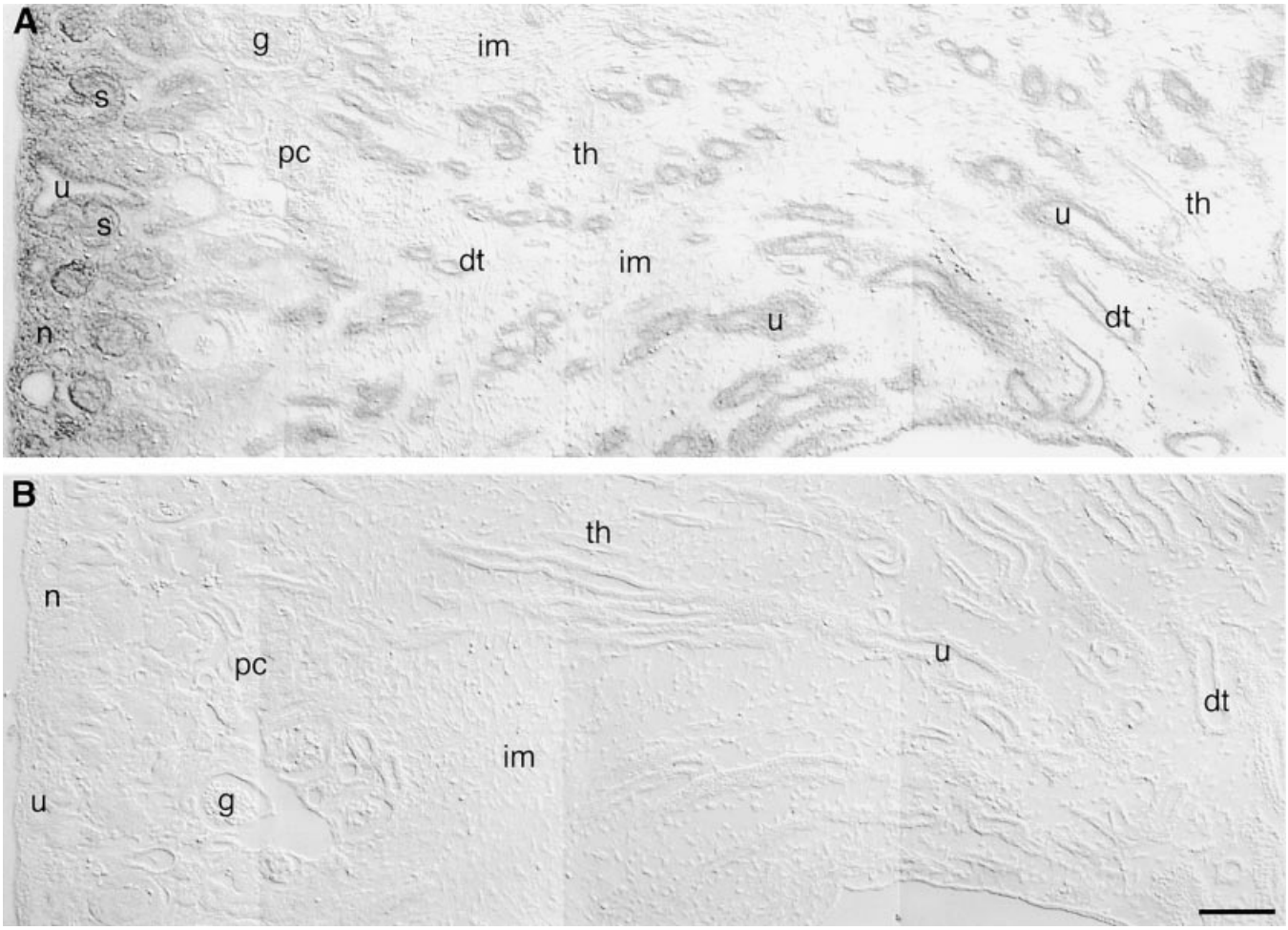

Fig. 4. Nonradioactive *in situ* hybridization of E20 rat metanephroi using biotin-UTP–labeled FGF1 cRNA probes. Photomicrographs were obtained using a differential interference contrast microscope (sections not counterstained). (*A*) Intense signal for FGF1 mRNA is localized in the developing nephrogenic zone (n). Strong signal is detected in ureteric epithelium (u) and S-shaped bodies (s), whereas only background levels of signal are seen in maturing glomeruli (g) and proximal convoluted tubules (pc). FGF1 mRNA is also detected in the medulla, in the ureteric epithelium (u) and in distal tubules (dt) of the immature loop of Henle. The thin undifferentiated epithlium (th) of the immature loop of Henle and the developing interstitium (im) did not contain FGF1 mRNA. (*B*) Adjacent section of metanephros hybridized with sense FGF1 cRNA probe (bar = 100 μm).

No immunostaining was observed in the interstitium (Fig. 6H), capillaries, or the endothelium of developing blood vessels, although weak immunostaining was observed in the tunica media of developing arteries. The localization of FGFR2 in rat metanephric structures is summarized in Table 4.

Fibroblast growth factor receptor 3

In the E20 metanephros, FGFR3 was also localized in the ureteric epithelium. However, unlike immunostaining for FGFR1 and FGFR2, this staining was restricted to ureteric epithelial cells in the nephrogenic zone, where branching occurs, and was not detected in more mature ureteric epithelium of the medulla, where widening of the developing papilla and collecting ducts occurs (Fig. 5K). In the nephrogenic zone, the nephrogenic mesenchyme was immunoreactive for FGFR3 (Fig. 6I). Immunostaining for FGFR3 was also localized in condensing mesenchyme (Fig. 6I), again suggesting these cells have the capacity to respond to a variety of FGFs. In developing nephrons, FGFR3 immunostaining was localized in vesicles, comma-shaped bodies, and S-shaped bodies (Fig. 6J). More intense immunoreactivity was observed in the middle limb (loop of Henle and distal tubule anlagen) of S-shaped bodies (Fig. 6J) and was maintained in these epithelia in more mature nephrons. Weak immunostaining was also localized in capillary loop and maturing-stage glomeruli (Fig. 6K). In maturing-stage glomeruli, immunoreactivity appeared to be in podocytes and endothelial cells but not in mesangial cells.

Immunostaining for FGFR3 changed with the development of the tubule anlagen of S-shaped bodies. Intense

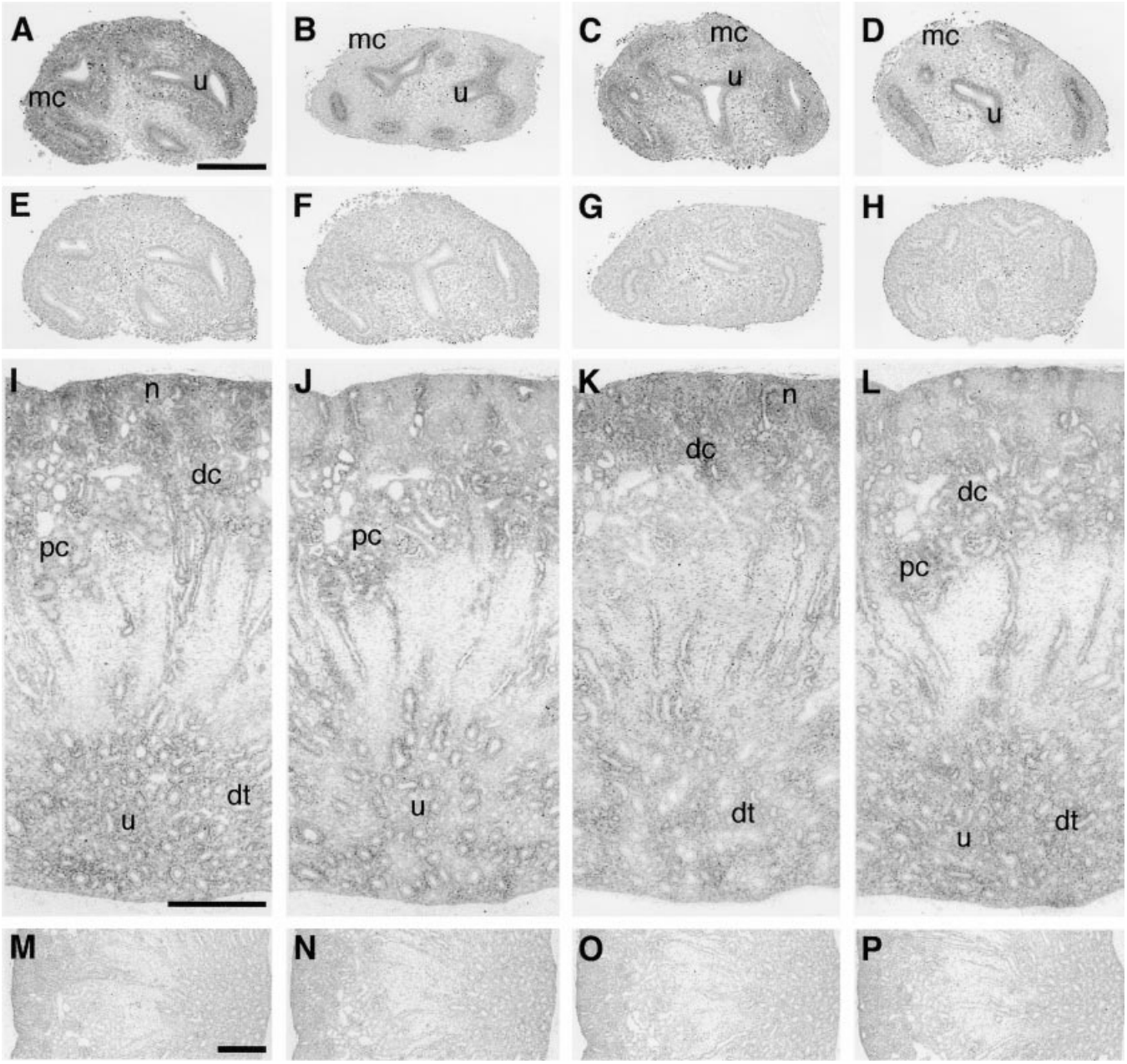

Fig. 5. Low-power micrographs of FGFR1, FGFR2, FGFR3, and FGFR4 protein localization in E15 (*A–H*) and E20 (*I–P*) rat metanephroi by immunohistochemistry. (A) FGFR1 immunoreactivity is localized to the ureteric epithelium (u) and condensing mesenchyme (mc). (B) FGFR2 immunostaining is detected in ureteric epithelium (u). (C) Immunoreactivity for FGFR3 is seen in the condensing mesenchyme (mc) and in ureteric epithelium (u). (D) FGFR4 immunoreactivity is present in ureteric epithelium (u). No immunoreactivity is seen in the preabsorption controls of E15 metanephroi for FGFR1 (D), FGFR2 (F), FGFR3 (G), or FGFR4 (H). (I) Immunostaining of FGFR1 in an E20 metanephros; in the developing cortex, the nephrogenic zone (n), proximal convoluted tubules (pc) and distal convoluted tubules (dc) are immunoreactive. All tubules in the developing medulla are immunoreactive for FGFR1, including ureteric epithelium (u) and distal straight tubules (dt). (J) FGFR2 immunoreactivity is localized to developing proximal convoluted tubules (pc) and ureteric epithelium (u). (K) Immunostaining of FGFR3 is present in the nephrogenic zone (n) of the cortex and in distal convoluted (dc) and distal straight (dt) epithelia. In the medulla, the ureteric epithelium is not immunoreactive for FGFR3. (L) Immunoreactivity for FGFR4 is localized to developing proximal (pc) and distal (dc) convoluted tubules in the cortex and to ureteric epithelium (u) and distal straight tubules (dt) in the medulla. No immunoreactivity is seen in the preabsorption controls of E20 metanephroi for FGFR1 (M), FGFR2 (N), FGFR3 (O), or FGFR4 (P). Bar in (A) = 100 μm (for A–H). Bar in (I) = 200 μm (for I–L). Bar in (M) = 200 μm (for M–P).

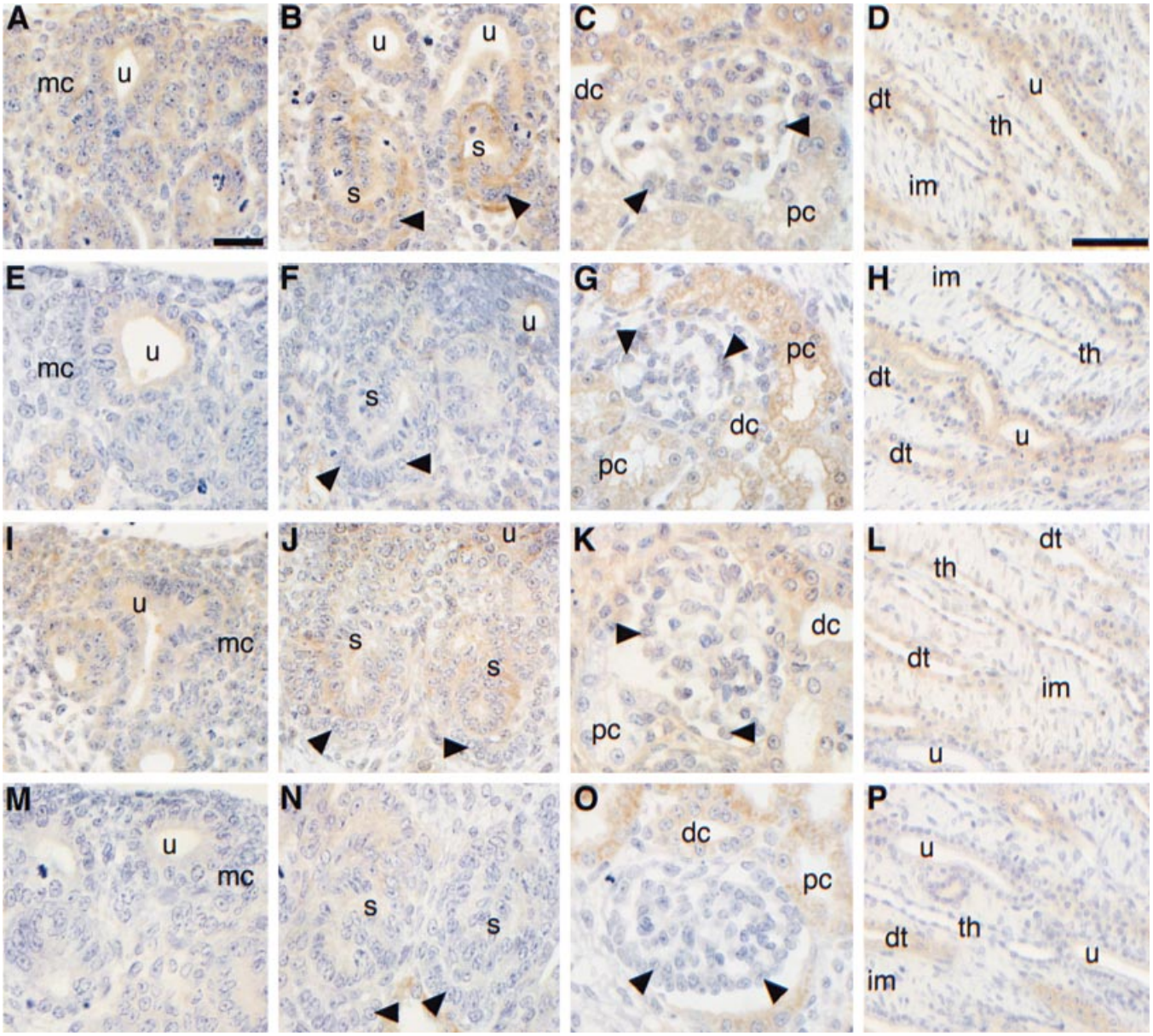

Fig. 6. High-power photomicrographs of FGFR1, FGFR2, FGFR3, and FGFR4 protein localization in E20 rat metanephroi by immunohistochemistry. (*A*) Immunoreactivity for FGFR1 is seen in ureteric epithelium (u) and mesenchymal condensate (mc). (*B*) Immunolocalization of FGFR1 is detected in S-shaped bodies (s), including the developing podocytes (arrowheads). (*C*) FGFR1 immunostaining is present in proximal (pc) and distal (dc) convoluted tubules and in all glomerular cells (podocytes are marked by arrowheads). (*D*) FGFR1 immunoreactivity is localized in the thin undifferentiated (th) and distal tubule (dt) epithelia of the immature loop of Henle. Staining is also present in the ureteric epithelium (u) of the medulla, but not in the interstitium (im). (*E*) Immunoreactivity for FGFR2 is seen in ureteric epithelium (u), but not in mesenchymal condensates (mc). (*F*) Faint staining is seen for FGFR2 in S-shaped bodies (s; podocytes are marked by arrowheads). (*G*) FGFR2 immunoreactivity is present in distal convoluted tubules (dc) and intense staining is seen in proximal convoluted tubules (pc). FGFR2 immunostaining in glomeruli is present in podocytes (arrowheads) and mesangium. (*H*) Immunolocalization for FGFR2 is detected in thin undifferentiated (th) and distal tubule (dt) epithelia of the immature loop of Henle and in the ureteric epithelium (u) of the medulla, but not in the interstitium (im). (*I*) In the nephrogenic zone, FGFR3 immunostaining is seen in ureteric epithelium (u) and mesenchymal condensates (mc). (*J*) S-shaped bodies (s) are immunoreactive for FGFR3 (podocytes are marked by arrowheads). (*K*) FGFR3 immunoreactivity is present in distal convoluted tubules (dc) but no staining is seen in proximal convoluted tubules (pc). In glomeruli, immunostaining for FGFR3 is present in podocytes (arrowheads) and endothelium. (*L*) FGFR3 immunostaining is seen in distal tubule epithelium (dt), and weak staining is present in thin undifferentiated epithelium (th) of the immature loop of Henle. Immunoreactivity for FGFR3 is also present in the medullary interstitium (im), but is not detected in the medullary ureteric epithelium (u). (*M*) Weak immunostaining for FGFR4 is seen in ureteric epithelium (u), but no staining is present in mesenchymal condensates (mc). (*N*) Weak immunostaining for FGFR4 is detected in S-shaped bodies (s) but not in the developing podocyte layer (arrowheads). (*O*) FGFR4 immunoreactivity is present in distal (dc) and proximal (pc) convoluted tubules. No immunoreactivity for FGFR4 is detected in glomeruli (podocytes are marked by arrowheads). (*P*) FGFR4 immunostaining is present in distal tubule epithelium (dt), with weak staining in ureteric epithelium (u). No FGFR4 immunoreactivity is detected in the thin undifferentiated epithelium (th) of the immature loop of Henle or in the medullary interstitium (im). Bar in (A) = 20 μm (for A–C, E–G, I–K, and M–O). Bar in (D) = 50 μm (for D, H, L, P).

Table 4. Summary of immunolocalization patterns for FGFR1, FGFR2, FGFR3, and FGFR4 in E20 rat metanephroi

Metanephric structure	FGFR1	FGFR2	FGFR3	FGFR4
Mesenchymal condensate	+	−	+	−
Comma-shaped body	+	±	+	±
S-shaped body	+	±	+	±
Capillary loop stage glomerulus	+	+	+	−
Maturing stage glomerulus	+	+	+	−
Proximal convoluted tubule	+	+	−	+
Distal convoluted tubule	+	+	+	+
Primitive loop of Henle	+	+	+	±
Proximal straight tubule	+	+	+	+
Thin undifferentiated epithelium	+	+	±	−
Distal tubule	+	+	+	+
Metanephric mesenchyme	+	−	+	−
Medullary interstitium	−	−	+	−
Ureteric epithelium: cortex (c), medulla (m)	c +, m +	c +, m +	c +, m −	c ±, m ±
Capillary endothelium and blood vessels	+	−	±	−

Symbols are: +, immunoreactive; ±, weak immunostaining; −, no immunostaining.

FGFR3 immunoreactivity was localized to developing distal tubules (Fig. 6K) but was not detected in proximal convoluted tubules. Immunostaining for FGFR3 was localized throughout the primitive loop of Henle; this localization was maintained in the immature loop of Henle, where immunoreactivity was detected in the thin undifferentiated epithelium and distal epithelium (Fig. 6L). Weak immunostaining for FGFR3 was observed in the interstitium (Fig. 6L), capillaries, the endothelium of developing blood vessels, and the tunica media of arteries. The localization of FGFR3 in rat metanephric structures is summarized in Table 4.

Fibroblast growth factor receptor 4

Immunoreactivity for FGFR4 was primarily detected in maturing nephron structures of the E20 metanephros (Fig. 5L). Weak immunostaining for FGFR4 was detected throughout the ureteric epithelium. No immunoreactivity was detected in the nephrogenic mesenchyme or in mesenchymal condensates (Fig. 6M). Weak immunostaining was detected in comma-shaped bodies and in the upper and middle limbs of S-shaped bodies (Fig. 6N). However, no staining was detected in the lower limb of S-shaped bodies or in developing or maturing glomeruli (Fig. 6 N, O).

The weak immunostaining observed in the tubule anlagen of the S-shaped bodies altered with tubule development. In maturing nephrons, FGFR4 was immunolocalized to proximal convoluted tubules with some cross-sections only weakly stained, and intense staining was detected in distal tubules (Fig. 6O). FGFR4 immunoreactivity was detected in the primitive loop of Henle. In the immature loop of Henle, FGFR4 was not detected in the thin undifferentiated epithelium but was detected in the distal ascending epithelium (Fig. 6P). No immunoreactivity for FGFR4 was detected in the interstitium (Fig. 6P), capillaries, or the endothelium or walls of developing blood vessels. The localization of FGFR4 in rat metanephric structures is summarized in Table 4.

DISCUSSION

This study has determined by RT-PCR that mRNAs for FGF1, FGF2, FGF3, FGF4, FGF5, FGF7, FGF8, FGF9, and FGF10 are expressed early (from at least E14) in rat metanephric development and continue to be expressed throughout metanephrogenesis. This large array of FGFs may interact with all seven functional FGFR variants throughout gestation, except FGFR3-IIIb, which is not expressed in rat metanephroi until E16. FGF6 is not expressed in developing rat metanephroi.

Previous studies have examined the expression of FGF1, FGF2, FGF7, and FGF8 in metanephroi. FGF1 is expressed in human fetal kidneys [10], and FGF2 mRNA is present in human fetal kidneys and was localized to tubular epithelia, mesangial cells, and surrounding mesenchyme [11]. FGF7 mRNA has been localized to the renal hilus of neonatal rat kidneys [12], and FGF8 mRNA has been localized to nephron elements in E14.5 and E15.5 mice [13, 14]. We have determined that in addition to mRNAs for FGF1, FGF2, FGF7, and FGF8, expression of FGF3, FGF4, FGF5, FGF9, and FGF10 mRNAs were also detected in metanephroi, and that all nine of these FGFs (FGF1 through FGF5 and FGF7 through FGF10) are expressed from at least E14 and throughout metanephrogenesis. We have also determined that FGF6 is not expressed by rat metanephroi at any stage of gestation.

Several FGF knockout mice have been generated, with varying severity of phenotypes. Knockout mice for FGF2 [36, 37], FGF3 [38], FGF5 [39], and FGF6 [40] do not have any obvious kidney defects, suggesting that these growth factors are not essential for kidney formation, or that other factors can compensate for their loss. FGF4

knockout mice are peri-implantation lethal; therefore, metanephrogenesis cannot be examined in these mice [41]. Interestingly, abrogation of FGFR2 IIIb signaling in dominant-negative receptor mutant mice results in severe kidney defects [42]. Of the well-documented FGFs, FGF1, FGF3, FGF7, and FGF10 are known to bind and signal through FGFR2 IIIb [19, 20]. As mentioned, FGF3 knockout mice show no obvious kidney phenotype; however, FGF7 knockout mice have 30% fewer nephrons than their wild-type littermates [43]. The mild phenotype seen in FGF7 knockout mice suggests that other FGFs, perhaps FGF1 or FGF10 or both, have a pivotal role in kidney development. A role for FGF10 in branching morphogenesis of the lung has been demonstrated in FGF10 knockout animals [44]; the kidneys of these mice were not described.

Fibroblast growth factor 1 can interact with the seven different FGFR variants [19], all of which were expressed in metanephroi. The localization of FGF1 mRNA did not overlap entirely with the localization of FGFR1 through FGFR4 protein observed in metanephroi. No expression of FGF1 mRNA was detected in proximal tubules, thin undifferentiated limbs of the immature loop of Henle, or the medullary interstitium. However, FGFR proteins were localized to these structures, indicating that other FGFs interact with these receptors.

We have previously shown that FGF1 and FGF2 protein are present in the epithelium of developing nephron elements, from the vesicle stage to S-shaped bodies, and in the developing glomerular mesangium of metanephroi, but not in mesenchymal condensates, endothelial cells, or the thin undifferentiated epithelium of the immature loop of Henle [15]. In this study, FGF1 mRNA had a similar distribution to FGF1 protein except the mRNA was also detected in mesenchymal condensates and maturing stage glomeruli. This difference may be due to differences in sensitivity of detection between immunohistochemistry and *in situ* hybridization. Alternatively, although the mRNA is present, there may be a delay in protein synthesis until the condensate has converted into epithelium. A similar delay in protein synthesis has been observed for the HSPG syndecan. Although syndecan mRNA is present throughout the mesenchyme of the early metanephros, syndecan protein is only present in induced mesenchyme around the ureteric bud [45]. In glomeruli, FGF1 mRNA levels appeared to decrease with maturation, whereas intense immunoreactivity for FGF1 protein was localized in the mesangium throughout glomerular development [15]. FGFs are heparin-binding proteins and may be synthesized early in glomerular formation and bind to the mesangial ECM, and therefore, FGF protein could be detected in the mesangium of maturing stage glomeruli.

Perantoni, Dove, and Karavanova showed that FGF2 could imitate the early events of an inductor tissue in cultured rat metanephric mesenchyme in that it induces mesenchymal condensation [9]. *In vivo*, FGF2 mRNA [11] and protein [15] were localized in the metanephric mesenchyme. The cells of this region either remain proliferative or differentiate into a condensate. FGFs may be involved in both of these functions by maintaining mesenchymal proliferation and by inducing mesenchymal condensation.

Several studies have examined the expression of FGFRs in metanephroi. Northern analysis of 17- to 18-week-old human fetal tissues showed that FGFR1, FGFR2, FGFR3, and FGFR4 are expressed in developing human kidneys [21]. Three splice variants of FGFR1 were detected by RT-PCR in rat metanephroi at E14, E17, and E20 [22], demonstrating that FGFR1 is expressed throughout metanephrogenesis. FGFR1, FGFR3, and FGFR4 were detected in E21 rat kidneys by RT-PCR [23]. These RT-PCR data are in agreement with Kim et al [22] and have extended the findings of Kee et al [23] by demonstrating expression of all four FGFRs and all seven FGFR variants throughout rat metanephrogenesis. The absence of FGFR3 IIIb at E14 and E15 suggests that this FGFR variant is not expressed until more mature structures have developed in the E16 rat metanephros.

Several studies have examined the localization of FGFR mRNAs in developing embryos by radioactive *in situ* hybridization [11, 24–26, 28, 29]. However, the major focus of these studies was not the developing kidney, and only brief descriptions of localization in metanephroi were provided. Close examination of the photomicrographs provided in these reports suggests that the FGFR protein localization results of this study are generally in agreement with these previous studies on FGFR mRNA localization.

Several studies have localized FGFR1 mRNA by *in situ* hybridization in developing rat and mouse kidneys [24–26]. Analysis of the photomicrographs provided in these studies shows that FGFR1 is expressed in collecting ducts, metanephric and condensing mesenchyme, vesicles, comma- and S-shaped bodies, developing glomeruli, and nephron tubules. The protein localization data of this study are in good agreement with these previous studies. In human metanephroi, FGFR1 protein and mRNA have been localized in renal tubules (including collecting ducts) and early nephron structures (comma- and S-shaped bodies); mRNA and protein were also detected in the surrounding stroma [11]. The antibody used by Gonzalez et al was made against the carboxy-terminus of human FGFR1, similar to the commercial antibody used in this study [11]. Although Gonzalez et al only provided a photomicrograph of a single glomerulus, the description of FGFR1 protein localization in human metanephroi matches that observed in rat metanephroi [11]. Targeted mutations of FGFR1 are embry-

onic lethal prior to kidney formation [46, 47]; therefore, the role of this receptor in metanephrogenesis cannot be determined in these mice.

The pattern of FGFR2 mRNA expression has been described in mouse embryos [25, 26]. FGFR2 was expressed in collecting ducts and some nephron tubules. However, the resolution of the radioactive *in situ* hybridization does not allow an accurate assessment of the exact tubule types expressing FGFR2. In addition to localization in ureteric epithelium, this study identified these FGFR2-expressing nephron tubules as proximal and distal convoluted tubules. Targeted disruption of FGFR2 IIIc is peri-implantation lethal [48]; therefore, the role of this receptor cannot be assessed in these mice. However, transgenic mice expressing a soluble dominant-negative FGFR2 IIIb have severe kidney defects [42]. The kidneys either failed to develop or formed a small disorganized organ with small glomeruli and enlarged vacuolated tubules. Markers of early nephron development were not expressed in severely affected mutant mice; the authors suggest that the dominant-negative receptor disrupted the induction of ureteric bud outgrowth and mesenchymal-epithelial conversion [42].

In situ hybridization studies on the expression pattern of FGFR4 in murine development has shown that it is expressed in a number of tissues including metanephroi [28, 29]. Within metanephroi, FGFR4 expression was found in collecting tubules at E14.5. Closer examination of the photomicrograph provided by Stark, McMahon, and McMahon shows that FGFR4 mRNA is expressed in ureteric epithelium in the cortex but not medulla and that developing nephron tubules also express FGFR4 mRNA, although developing glomeruli appear negative [28]. This expression pattern is similar to the protein localization described in this study, where nephron tubules were intensely immunoreactive for FGFR4, but no immunostaining in glomeruli and only weak immunostaining were found in ureteric epithelium. However, FGFR4 knockout mice are developmentally normal and do not have any overt organ defects [49].

Metanephric mesenchyme and mesenchymal condensates were immunoreactive for FGFR1 and FGFR3. The major ligands of these receptors are FGF1, FGF2, FGF4, and FGF9 [19]. All four ligands are expressed by metanephroi, but whether FGF4 or FGF9 are present in mesenchymal condensates has not yet been determined. FGFR3 IIIb is not expressed until E16, suggesting that the mesenchymal condensate localization of FGFR3 protein is due to the IIIc variant. Cytoplasmic immunostaining for FGF1 and FGF2 was observed in the epithelial vesicles that form from the mesenchymal condensates [15]. Weak immunoreactivity for FGFR2 and FGFR4 also emerged following conversion of mesenchyme to epithelium, suggesting these receptors play a role in nephron maturation.

Fibroblast growth factor receptor 3 mutant mice have skeletal dysplasias with elongation of the long bones [50, 51], whereas FGFR4 mutants are phenotypically normal [49]. Mice that are mutant for both FGFR3 and FGFR4 display phenotypes, which are not present in either FGFR3 or FGFR4 single mutants [49]; these mice display severe dwarfism and lung abnormalities. The broad distribution of FGFRs in metanephroi suggests that cooperativity between FGF ligands and the receptors is important for the formation and maturation of metanephroi.

Capillary loop stage glomeruli were immunoreactive for FGFR1, FGFR2, and FGFR3. This localization appeared to change with glomerular maturation. Although localization of reaction products from immunohistochemistry by light microscopy is not always accurate, differences in localization of these receptors in the three cell types of maturing stage glomeruli were evident. Maturing podocytes (glomerular epithelial cells) were immunoreactive for FGFR1, FGFR2, and FGFR3, whereas maturing mesangial cells were immunoreactive for FGFR1 and FGFR2 only, and maturing glomerular endothelial cells were immunoreactive for FGFR1 and FGFR3 only. These emerging differences in FGFR expression need to be confirmed at the electron microscope level before firm conclusions can be drawn. However, these results suggest that there may be differences in ligand responsiveness between different glomerular cell populations, and these differences may be important for glomerular maturation. Although all glomerular cells were immunoreactive for FGFR1, different cell types may express several functional variants, thus further refining the ligand interactions in these cells. We have recently described the expression pattern of FGFR IIIb and IIIc isoforms in adult rat glomeruli [32]. We found that the IIIc isoforms of FGFR1, FGFR2, and FGFR3, as well as FGFR4, were expressed in normal glomeruli, whereas the IIIb isoforms of FGFR1, FGFR2, and FGFR3 were not.

Ureteric epithelium expressed all four FGFRs. A notable difference in localization was observed for FGFR3, which was limited to cortical ureteric epithelium. This expression pattern suggests that FGFR3 may be more important for the mitogenic response of growing ureteric tips or for ureteric bud branching. No obvious kidney defects have been described in FGFR3 knockout mice [50, 51], suggesting that other FGFRs may compensate for the loss of FGFR3 or that cooperation between FGFR3 and another FGFR may be required.

Appropriate activation of FGFRs by FGFs requires HSPGs [16, 17]. During metanephric development, sulfated proteoglycans are initially produced at the ureteric bud tips and are subsequently found in basement membranes throughout the metanephros [18]. In mouse metanephric organ culture, inhibition of sulfated proteoglycan synthesis impairs ureteric bud branching [52–54].

A potential candidate HSPG for FGF activation in the developing kidney is syndecan-1 [45]. The localization of FGFRs, and in particular FGFR3 to ureteric bud tips, along with FGF1, FGF2, and HSPGs, shows that all of the essential components required for the formation of an appropriately active FGF/HSPG/FGFR signaling complex are in place for ureteric development. The array of ligands and receptors in developing nephron elements underscores the involvement of FGFs in formation or maturation of that structure and emphasizes the need for further localization studies for the other FGFs documented here.

In summary, we have used RT-PCR to determine that FGF1 through FGF5, FGF7 through FGF10, and FGFR1 through FGFR4 are expressed from E14 to E21 in the developing rat metanephros, and that all seven functional FGFR variants are expressed in metanephroi. We have also used immunohistochemistry to determine that FGFR proteins are localized in a distinct pattern in developing rat metanephroi, which alters with maturation of different nephron segments. The expression and discrete localization of FGFRs throughout metanephrogenesis suggest that FGFRs and their ligands may be important factors in kidney development and maturation. This study had provided the basis for further studies into the actions of FGFs in metanephroi. Future studies are planned where metanephric organ culture will be used to investigate the actions of those FGFs that we have identified as present in developing metanephroi.

ACKNOWLEDGMENTS

This work was supported by a grant from the National Health and Medical Research Council (NHMRC), Australia. B. Cancilla acknowledges receipt of a Dora Lush Biomedical Postgraduate scholarship from the NHMRC.

Reprint requests to John F. Bertram, Ph.D., Department of Anatomy, Monash University, Clayton, Victoria 3168, Australia.
E-mail: John.Bertram@med.monash.edu.au

REFERENCES

1. Saxen L: *Organogenesis of the Kidney.* London, Cambridge University Press, 1987
2. Neiss WF: Histogenesis of the loop of Henle in the rat kidney. *Anat Embryol* 164:315–330, 1982
3. Hogan BLM: Bone morphogenetic proteins: Multifunctional regulators of vertebrate development. *Genes Dev* 10:1580–1594, 1996
4. Betsholtz C, Raines EW: Platelet-derived growth factor: A key regulator of connective tissue cells in embryogenesis and pathogenesis. *Kidney Int* 51:1361–1369, 1997
5. Sariola H, Sainio K: The tip-top branching ureter. *Curr Opin Cell Biol* 9:877–884, 1997
6. Woolf AS, Cale CM: Roles of growth factors in renal development. *Curr Opin Nephrol Hypertens* 6:10–14, 1997
7. Nishimura T, Utsunomiya Y, Hoshikawa M, Ohuchi H, Itoh N: Structure and expression of a novel human FGF, FGF-19, expressed in the fetal brain. *Biochim Biophys Acta* 1444:148–151, 1999
8. Baird A, Bohlen P: Fibroblast growth factors, in *Peptide Growth Factors and Their Receptors Handbook of Experimental Pharmacology*, edited by Sporn MB, Roberts AB, Berlin, Springer-Verlag, 1990, pp 369–418
9. Perantoni AO, Dove LF, Karavanova I: Basic fibroblast growth factor can mediate the early inductive events in renal development. *Proc Natl Acad Sci USA* 92:4696–4700, 1995
10. Wang W-P, Lehtoma K, Varban ML, Krishnan I, Chiu I-M: Cloning of the gene coding for human class 1 heparin-binding growth factor and its expression in fetal tissues. *Mol Cell Biol* 9:2387–2395, 1989
11. Gonzalez AM, Hill DJ, Logan A, Maher PA, Baird A: Distribution of fibroblast growth factor (FGF)-2 and FGF receptor-1 messenger RNA expression and protein presence in the mid-trimester human fetus. *Pediatr Res* 39:375–385, 1996
12. Ichimura T, Finch PW, Zhang G, Kan M, Stevens JL: Induction of FGF-7 after kidney damage: A possible paracrine mechanism for tubule repair. *Am J Physiol* 271:F967–F976, 1996
13. Crossley PH, Martin GR: The mouse Fgf8 gene encodes a family of polypeptides and is expressed in regions that direct outgrowth and patterning in the developing embryo. *Development* 121:439–451, 1995
14. Mahmood R, Bresnick J, Hornbruch A, Mahony C, Morton N, Colquhoun K, Martin P, Lumsden A, Dickson C, Mason I: A role for FGF-8 in the initiation and maintenance of vertebrate limb bud outgrowth. *Curr Biol* 5:797–806, 1995
15. Cancilla B, Cauchi J, Key B, Nurcombe V, Alcorn D, Bertram JF: Immunolocalization of fibroblast growth factor-1 and -2 in the embryonic rat kidney. *Nephrology* 2:167–174, 1996
16. Givol D, Yayon A: Complexity of FGF receptors: Genetic basis for structural diversity and functional specificity. *FASEB J* 6:3362–3369, 1992
17. McKeehan WL, Wang F, Kan M: The heparan sulfate-fibroblast growth factor family: Diversity of structure and function. *Prog Nucleic Acid Res Mol Biol* 59:135–176, 1998
18. Kanwar YS, Carone FA, Kumar A, Wada J, Ota K, Wallner EI: Role of extracellular matrix, growth factors and proto-oncogenes in metanephric development. *Kidney Int* 52:589–606, 1997
19. Ornitz DM, Xu J, Colvin JS, McEwen DG, MacArthur CA, Coulier F, Gao G, Goldfarb M: Receptor specificity of the fibroblast growth factor family. *J Biol Chem* 271:15292–15297, 1996
20. Xu X, Weinstein M, Li C, Naski M, Cohen RI, Ornitx DM, Leder P, Deng C: Fibroblast growth factor receptor 2 (FGFR2)-mediated reciprocal regulation loop between FGF8 and FGF10 is essential for limb induction. *Development* 125:753–765, 1998
21. Partanen J, Makela TP, Eerola E, Korhonen J, Claesson-Welsh L, Alitalo K: FGFR-4, a novel acidic fibroblast growth factor receptor with a distinct expression pattern. *EMBO J* 10:1347–1354, 1991
22. Kim EG, Kwon HM, Burrow CR, Ballerman BJ: Expression of rat fibroblast growth factor receptor 1 as three splicing variants during kidney development. *Am J Physiol* 264:F66–F73, 1993
23. Kee N, McTavish AJ, Papillon J, Cybulsky AV: Receptor protein tyrosine kinases in perinatal developing rat kidney. *Kidney Int* 52:309–317, 1997
24. Wanaka A, Milbrandt J, Johnson EM: Expression of FGF receptor gene in rat development. *Development* 111:455–468, 1991
25. Orr-Urtreger A, Givol D, Yayon A, Yarden Y, Lonai P: Developmental expression of two murine fibroblast growth factor receptors, flg and bek. *Development* 113:1419–1434, 1991
26. Peters KG, Werner S, Chen G, Williams LT: Two FGF receptor genes are differentially expressed in epithelial and mesenchymal tissues during limb formation and organogenesis in the mouse. *Development* 114:233–243, 1992
27. Wuechner C, Sandberg-Nordqvist A-C, Winterpacht A, Zabel B, Schalling M: Developmental expression of splicing variants of fibroblast growth factor receptor 3 (FGFR3) in mouse. *Int J Dev Biol* 40:1185–1188, 1996
28. Stark KL, McMahon JA, McMahon AP: FGFR-4, a new member of the fibroblast growth factor receptor family, expressed in the definitive endoderm and skeletal muscle lineages of the mouse. *Development* 113:641–651, 1991
29. Korhonen J, Partanen J, Alitalo K: Expression of FGFR-4 mRNA in developing mouse tissues. *Int J Dev Biol* 36:323–329, 1992

30. Nurcombe V, Ford MD, Wildschut JA, Bartlett PF: Developmental regulation of neural response to FGF-1 and FGF-2 by heparan sulfate proteoglycan. *Science* 260:103–106, 1993
31. El-Husseini AE-D, Paterson JA, Myal Y, Shiu RPC: PCR detection of the rat brain basic fibroblast growth factor (bFGF) mRNA containing a unique 3′ untranslated region. *Biochim Biophys Acta* 1131:314–316, 1992
32. Ford MD, Cauchi J, Greferath U, Bertram JF: Expression of fibroblast growth factors and their receptors in rat glomeruli. *Kidney Int* 51:1729–1738, 1997
33. Sambrook J, Fritsch EF, Maniatis T: *Molecular Cloning: A Laboratory Manual.* New York, Cold Spring Harbor Press, 1989
34. Key B, Treloar HB, Wangerek L, Ford MD, Nurcombe V: Expression and localization of FGF-1 in the developing rat olfactory system. *J Comp Neurol* 366:197–206, 1996
35. Cancilla B, Risbridger GP: Differential localization of fibroblast growth factor receptor-1-2-3 and -4 in fetal, immature and adult rat testes. *Biol Reprod* 58:1138–1145, 1998
36. Dono R, Texido G, Dussel R, Ehmke H, Zeller R: Impaired cerebral cortex development and blood pressure regulation in FGF-2-deficient mice. *EMBO J* 17:4213–4225, 1998
37. Ortega S, Ittmann M, Tsang SH, Ehrlich M, Basilico C: Neuronal defects and delayed wound healing in mice lacking fibroblast growth factor 2. *Proc Natl Acad Sci USA* 95:5672–5677, 1998
38. Mansour SL, Goddard JM, Capecchi MR: Mice homozygous for a targeted disruption of the proto-oncogene int-2 have developmental defects in the tail and inner ear. *Development* 117:13–28, 1993
39. Hebert JM, Rosenquist T, Gotz J, Martin GR: FGF5 as a regulator of the hair growth cycle: Evidence from targeted and spontaneous mutations. *Cell* 78:1017–1025, 1994
40. Floss T, Arnold H-H, Braun T: A role for FGF-6 in skeletal muscle regeneration. *Genes Dev* 11:2040–2051, 1997
41. Feldman B, Poueymirou W, Papaioannou VE, Dechiara TM, Goldfarb M: Requirement of FGF-4 for postimplantation mouse development. *Science* 267:246–249, 1995
42. Celli G, Larochelle JW, Mackem S, Sharp R, Merlino G: Soluble dominant-negative receptor uncovers essential roles for fibroblast growth factors in multi-organ induction and patterning. *EMBO J* 17:1642–1655, 1998
43. Qiao J, Uzzo R, Obara-Ishihara T, Degenstein L, Fuchs E, Herzlinger D: FGF-7 modulates ureteric bud growth and nephron number in the developing kidney. *Development* 126:547–554, 1999
44. Sekine K, Ohuchi H, Fujiwara M, Yamasaki M, Yoshizawa T, Sato T, Yagishita N, Matsui D, Koga Y, Itoh N, Kato S: Fgf10 is essential for limb and lung formation. *Nat Genet* 21:138–141, 1999
45. Vainio S, Jalkanen M, Bernfield M, Saxen L: Transient expression of syndecan in mesenchymal cell aggregates of the embryonic kidney. *Dev Biol* 152:221–232, 1992
46. Deng C, Wynshaw-Boris A, Shen MM, Daugherty C, Ornitz DM, Leder P: Murine FGFR-1 is required for early post-implantation growth and axial organization. *Genes Dev* 8:3045–3057, 1994
47. Yamaguchi TP, Harpal K, Henkemeyer M, Rossant J: *fgfr-1* is required for embryonic growth and mesodermal patterning during mouse gastrulation. *Genes Dev* 8:3032–3044, 1994
48. Arman E, Haffner-Krausz R, Chen Y, Heath JK, Lonai P: Targeted disruption of fibroblast growth factor (FGF) receptor 2 suggests a role for FGF signaling in pregastrulation mammalian development. *Proc Natl Acad Sci USA* 95:5082–5087, 1998
49. Weinstein M, Xu X, Ohyama K, Deng C-X: FGFR-3 and FGFR-4 function cooperatively to direct alveogenesis in the murine lung. *Development* 125:3615–3623, 1998
50. Colvin SJ, Bohne BA, Harding GW, McEwen DG, Ornitz DM: Skeletal overgrowth and deafness in mice lacking fibroblast growth factor receptor 3. *Nat Genet* 12:390–397, 1996
51. Deng C, Wynshaw-Boris A, Zhou F, Kuo A, Leder P: Fibroblast growth factor receptor 3 is a negative regulator of bone growth. *Cell* 84:911–921, 1996
52. Platt JL, Brown DM, Granlund K, Oegema TR, Klein DJ: Proteoglycan metabolism associated with mouse metanephric development: Morphologic and biochemical effects of β-D-xyloside. *Dev Biol* 123:293–306, 1987
53. Lelongt B, Makino H, Daleki TM, Kanwar YS: Role of proteoglycans in renal development. *Dev Biol* 128:256–276, 1988
54. Davies J, Lyon M, Gallagher J, Garrod D: Sulfated proteoglycan is required for collecting duct growth and branching but not nephron formation during kidney development. *Development* 121:1507–1517, 1995